JOURNAL OF APPLIED PHYSICS **117**, 034305 (2015)

A semi-empirical model relating micro structure to acoustic properties of bimodal porous material

Shahrzad Ghaffari Mosanenzadeh,[1] Olivier Doutres,[2] Hani E. Naguib,[1,a)] Chul B. Park,[1] and Noureddine Atalla[2]
[1]*Department of Mechanical and Industrial Engineering, University of Toronto, Toronto, Canada M5S 3G8*
[2]*Groupe d'Acoustique de Vibrations de l'Universite' de Sherbrooke, Sherbrooke, Quebec, Canada J1K 2R1*

(Received 29 August 2014; accepted 19 December 2014; published online 16 January 2015)

Complex morphology of open cell porous media makes it difficult to link microstructural parameters and acoustic behavior of these materials. While morphology determines the overall sound absorption and noise damping effectiveness of a porous structure, little is known on the influence of microstructural configuration on the macroscopic properties. In the present research, a novel bimodal porous structure was designed and developed solely for modeling purposes. For the developed porous structure, it is possible to have direct control on morphological parameters and avoid complications raised by intricate pore geometries. A semi-empirical model is developed to relate microstructural parameters to macroscopic characteristics of porous material using precise characterization results based on the designed bimodal porous structures. This model specifically links macroscopic parameters including static airflow resistivity (σ), thermal characteristic length (Λ'), viscous characteristic length (Λ), and dynamic tortuosity (α_∞) to microstructural factors such as cell wall thickness $(2t)$ and reticulation rate (R_w). The developed model makes it possible to design the morphology of porous media to achieve optimum sound absorption performance based on the application in hand. This study makes the base for understanding the role of microstructural geometry and morphological factors on the overall macroscopic parameters of porous materials specifically for acoustic capabilities. The next step is to include other microstructural parameters as well to generalize the developed model. In the present paper, pore size was kept constant for eight categories of bimodal foams to study the effect of secondary porous structure on macroscopic properties and overall acoustic behavior of porous media. © *2015 AIP Publishing LLC*.
[http://dx.doi.org/10.1063/1.4905834]

I. INTRODUCTION

Due to the complicated microstructure of open cell porous media, engineering design of such material for optimum acoustic performance can be rather intricate and is still an open problem in the field. While existing acoustic models relate sound absorption properties of porous media to macro structural characteristics with acceptable accuracy, there is an imminent need for understanding the effect of micro structure on physical properties and overall acoustic behavior of open cell porous media. Different approaches have been proposed in the literature to link micro and macro properties of porous media. For more complicated cell structures, empirical methods were developed. These methods use direct measurement results to relate acoustic performance to micro structure of that specific class of material.[1–5] In recent years, scaling laws were employed to develop analytical models of propagation of wave inside the microstructure,[6–10] as well as numerical homogenization based on a representative unit cell.[7,11–14]

Advances in technology make it possible to apply rather computationally intensive models to predict propagation of wave in porous media. It is equally important to be able to closely design the micro structure and control every detail to decrease the number of micro structural factors affecting the final macroscopic behavior. Controlled design of microstructure provides the opportunity to study the effect of each morphological parameter separately. As reported in a previous study,[15] a rather innovative foam fabrication method involving particulate leaching has been used to fabricate highly porous bimodal structures. These foams are fabricated from bio-based polymers, Polylactide (PLA), and Polyethylene Glycol (PEG), for sound absorption applications and acoustic modeling purposes. Particulate leaching method was employed to fabricate the bimodal foams with direct control on cell morphology of the resulting porous structure. The foam fabrication method is explained in details by Ghaffari *et al.*[15] using sodium chloride as the main particulates and PEG micro powder as secondary particulates in a PLA matrix. Since PEG is soluble in PLA, final removal of PEG micro particles leaves micro pores into the foam structure, which makes the secondary porous configuration as illustrated in Figure 1. Polymers used in these foams are completely bio-based and environmentally friendly, therefore successful development of such acoustic absorbers solves the environmental concerns raised by existing petrochemical based noise controllers.

Present paper reports a semi-empirical model developed to relate micro structural properties to macroscopic characteristics of eight bimodal porous structures designed through

a)Author to whom correspondence should be addressed. Tel.: (416) 978-7054. Fax: (416) 978-7753. Electronic mail: naguib@mie.utoronto.ca

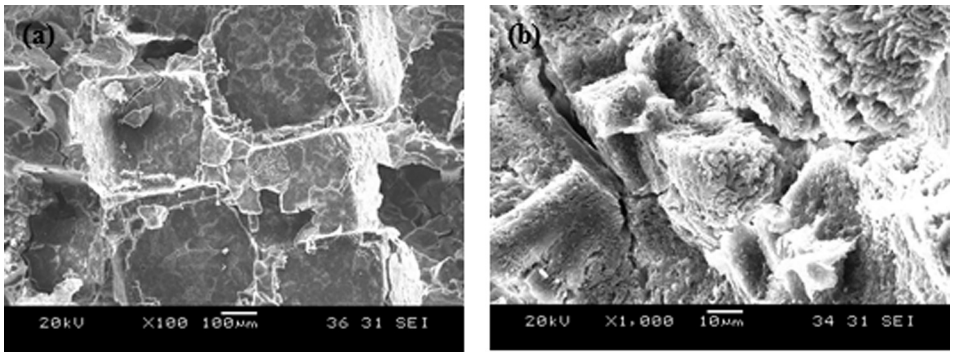

FIG. 1. SEM micrographs of foams with 15% PLA and PEG/PLA equal to 0.3 with (a) magnification of 100 and (b) magnification of 1000.

previous research.[15] For this purpose, a representative unit cell is considered based on the interconnected cell structure under study. A similar approach has been presented by Doutres *et al.*[9] for polyurethane foams.

In this context, the porous structure is considered to be homogeneous and have a rigid frame, which remains motionless in contact with sound wave. The rigid frame assumption is valid in the present case since the saturating fluid is air and PLA foam has a rigid matrix. Normal incidence sound absorption coefficient (α) of the foams is measured directly by two microphone impedance tube. Porosity $(\varnothing)$ and static airflow resistivity (σ) are measured directly as structural properties. A fluid equivalent model based on the work of Johnson-Champoux-Allard[16] is applied using the direct characterization results to obtain the three non-acoustic properties, tortuosity (α_∞), viscous characteristic length (Λ), and thermal characteristic length (Λ').

In order to link microstructural properties of the porous media to macroscopic characteristics, a representative cell geometry based on the interconnected cubic cells is assumed. Equations are developed to relate flow resistivity, thermal and viscous characteristic lengths to two microstructural factors named reticulation rate (R_w) and half cell wall thickness (t). Sections II and III discuss the porous structure under study and the developed semi-empirical model.

II. FOAM CHARACTERIZATION

A. Cell morphology

Scanning electronic microscope was used to study the cellular structure of bimodal PLA foams. Figure 1(a) shows the cell morphology of bimodal foam with 15 wt. % PLA. Overall cell structure has cubic geometry due to the shape of particulates used to fabricate the foams. This rather simple cell geometry is ideal for modeling purposes and to study the link between micro structure and overall acoustic properties of porous media. Figure 1(b) shows the foam matrix with higher magnification to demonstrate the secondary porous structure extending through the foam by increasing the amount of water soluble polymer. These micro pores form the bimodal foam structure.[15] Since PEG is soluble in PLA, it melts during the molding process and penetrates into PLA making micro openings in the foam skeleton after leaching. Average cell size for all foam samples measured in the diagonal direction was in the range of 350 (± 30) μm and cell density of foams with 15% PLA was reported to be 11×10^4 $(\pm 14\,000)$ cell/cm^3 and for foams with 10% PLA was 20×10^4 $(\pm 16\,000)$ cell/cm^3.[15]

Based on the cell morphology, bimodal foams are modeled as a network of interconnected cubic cells as shown in Figure 2. The microstructure of PLA foams is characterized by cell size C, cell length l, cell wall thickness $2t$, and the reticulation rate R_w. The representative unit cell is perforated to account for the micro openings in the cell wall. Size and position of the perforations are arbitrary and indicate the high porosity of the foam structure.

The concept of "Reticulation Rate" at the cell size scale is defined as the ratio of the open surface to the total cell wall surface. In open cell porous material, the structure is called "*fully reticulated*" if the interconnectivity between cells is maximum in which case the cells will be connected by thin struts. For the case of fully reticulated foams, the limit of R_w is close to 1. If some of the pores are closed or partially closed by thin membranes, the material is called "*partially reticulated*."

Bimodal PLA foams fabricated in this research are partially reticulated. Different factors such as non-homogeneity of the foam material affect porosity and reticulation rate of foams.[17,18] In the present paper, reticulation rate R_w will be used as a microstructural parameter to apply the effect of processing parameters into the proposed model. Cell length and cell wall thickness can be estimated from SEM images and porosity measurements. Reticulation rate of bimodal PLA foams can be estimated from SEM micrographs and thermal characteristic length results. The first step is to estimate the geometrical values in the cell size level from the previously characterized macroscopic properties as well as SEM micrographs.

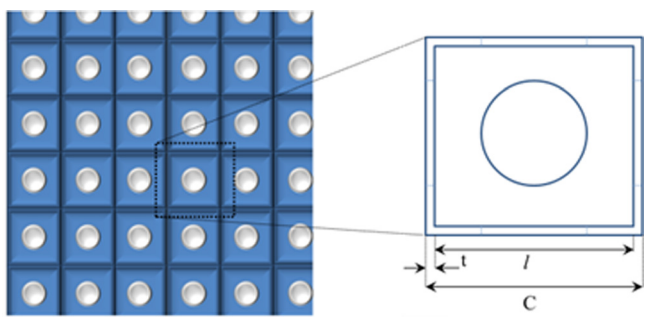

FIG. 2. Configuration of the representative unit cell.

B. Structural properties

Five main structural properties of porous material including porosity $\varnothing\,[\%]$, static air flow resistivity $\sigma\left[\frac{N.s}{m^4}\right]$, dynamic tortuosity α_∞, and viscous and thermal characteristic lengths $\Lambda\,[\mu m]$, and $\Lambda'[\,\mu m]$ are studied in the present paper.

Porosity and static air flow resistivity of the biobased foams were measured directly. Due to structural limitations, direct measurement of tortuosity and characteristic lengths was not possible without damaging the foam structure. For this purpose, indirect methods were employed by FOAMX[19,20] code based on the fluid equivalent model of Johnson-Champoux-Allard (JCA model). This method estimates dynamic tortuosity and characteristic lengths of open cell foams based on direct measurements of porosity, air flow resistivity, and normal incidence sound absorption coefficient.[19] The JCA model considers the porous frame to be rigid and not subjected to structural deformation by the energy of the sound wave.

Porosity was measured based on ASTM D6226 standard by gas pycnometer. Porosity of foams with 15% PLA is 82% ($\pm$1.2) and for foams with 10% PLA is 88% ($\pm$1.8).[15] The static airflow resistivity was measured according to the ASTM C522 standard. Table I summerises the evaluated values of structural properties of bimodal foams directly measured and determind by Johnson-Champoux-Allard model.

C. Acoustic absorption

Normal incidence sound absorption coefficient of biobased foams was measured by two microphone impedance tubes in accordance to ISO-10534-2 standard. An inverse method based on Johnson-Champoux-Allard equivalent fluid model was applied to the bimodal foams. This method uses the direct characterization of acoustic absorption coefficient, porosity, and static airflow resistivity to determine three macroscopic structural properties (dynamic tortuosity, viscous characteristic length, and thermal characteristic length) by solving an optimization problem. To apply the JCA model, four acoustic absorption curves measured directly for different foam samples were used for each category. The optimized solution with the best fit to the acoustic absorption curves determines the estimation for tortuosity and characteristic lengths. The accuracy of direct measurements for acoustic absorption, porosity, and flow resistivity is very important in successful determination of estimated values. Figure 3 shows the results of adjusting the simulation to reproduce the measured sound absorption coefficient for bimodal foams. As evident from the graphs, the results of inverse method are in good agreement with direct measurements of normal incident absorption coefficient.[19]

As observed from theoretical modeling results listed in Table I, the value of tortuosity remains relatively constant by increasing the water soluble polymer content. The formation of bimodal structure does not affect tortuosity; this can be explained by a closer look at the description of tortuosity. It can be shown that for an ideal nonviscous flow, effective density of the fluid is related to tortuosity by[16]

TABLE I. Structural properties of bimodal PLA foams.

	10% PLA				15% PLA			
Foam material	0% PEG	10% PEG	20% PEG	30% PEG	0% PEG	10% PEG	20% PEG	30% PEG
Porosity ($\varnothing$)	88.06 ($\pm$0.74)	88.34 ($\pm$0.33)	87.55 ($\pm$0.79)	86.96 ($\pm$1.77)	81.74 ($\pm$0.48)	82 ($\pm$1.24)	82.17 ($\pm$0.7)	82.14 ($\pm$0.56)
Flow resistivity (N.s/m^4)	1.2×10^5 ($\pm$10800)	8×10^4 ($\pm$11200)	6.7×10^4 ($\pm$5600)	7.4×10^4 ($\pm$12000)	1.3×105 ($\pm$13000)	1.1×10^5 ($\pm$13200)	1.0×105 ($\pm$8000)	9.8×104 ($\pm$14700)
Tortuosity α_∞	1.26 ($\pm$0.4)	1.26 ($\pm$0.05)	1.2 ($\pm$0.05)	1.21 ($\pm$0.16)	1.59 ($\pm$0.55)	1.48 ($\pm$0.47)	1.41 ($\pm$0.82)	1.44 ($\pm$0.41)
Viscous length Λ (μm)	5.7 ($\pm$1.5)	12.4 ($\pm$0.5)	11.8 ($\pm$2.5)	10.1 ($\pm$1.5)	5.2 ($\pm$2.1)	7.3 ($\pm$2.8)	8.1 ($\pm$5.2)	8.3 ($\pm$2.5)
Thermal length Λ' (μm)	74.5 ($\pm$19.6)	149.7 ($\pm$17.1)	166.7 ($\pm$17.7)	167.4 ($\pm$30.5)	81.1 ($\pm$18.7)	124.7 ($\pm$22.8)	153.4 ($\pm$45.3)	159.7 ($\pm$23.3)

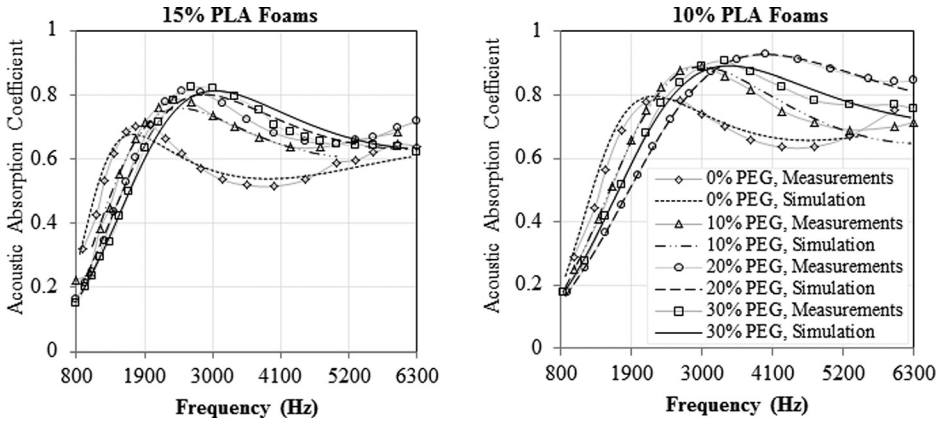

FIG. 3. JCA model simulation compared to direct measurement of normal incidence absorption coefficient.

$$\rho = \alpha_\infty \rho_0 , \tag{1}$$

where ρ_0 is the density of saturating fluid and α_∞ is the limit of dynamic tortuosity when ω tends to infinity. Consider a flow of nonviscous fluid with microscopic velocity at any point N in the fluid denoted by $v_m(N)$ and macroscopic velocity by $v(N_0)$. The macroscopic velocity can be obtained by averaging the microscopic velocity over a representative elementary volume V around N_0[16]

$$v(N_0) = \langle v_m(N) \rangle_V . \tag{2}$$

The tortuosity is defined by the relation[16]

$$\alpha_\infty = \frac{\langle v_m^2(N) \rangle_V}{v^2(N_0)} . \tag{3}$$

Therefore, from the macroscopic velocity point of view, the nonviscous fluid can be replaced by a fluid of density $\alpha_\infty \rho_0$. The value of tortuosity is an intrinsic property of the porous frame that depends on the micro-geometry.[16] A tortuosity value larger than 1 is due to the dispersion of the microscopic velocity in Eq. (3). This dispersion can be the result of variations of the diameters of the pores. For example, assume a material with identical pores parallel to the direction of propagation, made up of alternating cylinders as shown in Figure 4.

Even for the case of nonviscous fluids, description of inertial forces and evaluation of α_∞ by Eq. (3) is very complicated at the junction of the two cylinders. By assuming constant velocities in each cylinder, Atalla *et al.*[16] proposed the following approximation for evaluating the tortuosity

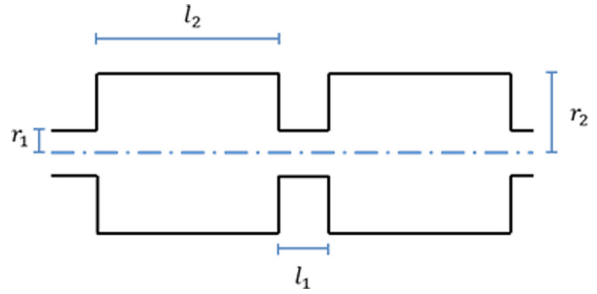

FIG. 4. Schematic of primary and secondary pores.

$$\alpha_\infty = \frac{(l_1 S_2 + l_2 S_1)(l_1 S_1 + l_2 S_2)}{(l_1 + l_2)^2 S_1 S_2} . \tag{4}$$

Here, S_2 and S_1 are the cross section area of large and small pores, respectively. For the bimodal structure, the main pores are the larger cell dimensions, while the micro pores resemble the smaller voids caused by cracks. If the order of magnitude of small pores is much less than large pores as is the case here, then the limit of Eq. (4) is

$$\alpha_\infty \cong \frac{l_1 S_2 \times l_2 S_2}{(l_1 + l_2)^2 S_1 S_2} + \frac{l_2 S_1 \times l_2 S_2}{(l_1 + l_2)^2 S_1 S_2} \cong \frac{l_1 S_2}{l_2 S_1} + 1. \tag{5}$$

Addition of water soluble polymer makes micro openings in the cell wall, which can be represented by r_1 in Figure 4. A minor decrease in the tortuosity values was observed by adding the water soluble polymer. Considering Eq. (5), by increasing the water soluble polymer content, the crack area S_1 will increase, while the thickness l_1 remains unchanged, which explains the slight decrease in tortuosity values. In the case of increased cell wall thickness (by using higher polymer content in the foam structure), on the other hand, l_1 increases more significantly, while S_1 remains unchanged for any water soluble polymer content, resulting in higher tortuosity values for foams with 15% PLA than the ones with 10% PLA. As observed from SEM images, the dimension l_1 is increased by 60% from foams with 10% PLA to the ones with 15% PLA. The effect of this increase was observed on the tortuosity values, increasing tortuosity from an average of about 1.2 to 1.5.

Based on the inverse characterization results, values of thermal characteristic length increase by increasing the PEG content. In other words, as the bimodal structure extends throughout the foam, surface area of the cell structure which is in contact with the saturating fluid decreases. This decrease happens due to more openings made in the cell walls caused by cracks, which in turn decreases the wet surface or the cell surface in contact with the saturating fluid. Evidently, higher polymer content makes thicker cell walls and more solid foam structure. This results in fewer openings in the cell walls and, therefore, bimodal foams with higher polymer content generally have lower values of thermal length.

Viscous characteristic length increases by the formation of the secondary porous structure inside PLA foams. This was

expected since viscous characteristic length reflects the importance of airflow in the pores and, thus, represents the smaller pores due to the high air particle velocity at these locations. Viscous length is inversely correlated to flow resistivity of porous structure. Formation of bimodal structure decreases flow resistivity, which results in higher values of viscous characteristic length. Decreasing the polymer content reduces the flow resistivity as well which is the reason for higher viscous length of foams with 10% PLA compared to foams with 15% PLA.

III. LINK MICROSTRUCTURE TO MACROSCOPIC PROPERTIES

To be able to apply analytical methods to any porous medium for prediction of acoustic behaviour, the structure of the material must be homogenuous. Homogeneity of the foam samples was tested in impedance tube by comparing the acoustic absorption curves from both sides of foams. As explained in detail by Mosanenzadeh *et al.*,[19] the two curves are identical, which indicates the homogeneity of the fabricated porous structures. Homogeneity of foam samples improves by increasing the amount of water soluble polymer due to decreased flow resistivity.

A. Estimation of cell length and cell wall thickness

As obtained from SEM micrographs, the average cell size of PLA foams is in the range of 220 μm because of the salt particles size. Due to the simple geometry of the cells, cell wall thickness can be estimated from porosity measurements with high accuracy. Porosity is a purely geometrical macroscopic parameter and can be defined as the ratio of the fluid volume V_f to the total volume V_t, as given by Gibson and Ashby.[6] For highly porous materials

$$\phi = \frac{V_f}{V_t}. \tag{6}$$

For cubic cells shown in Figure 2 and without taking into account the effect of the small perforations, it can simply be written as

$$\phi = \frac{V_f}{V_t} = \frac{l^3}{(l+2t)^3}, \tag{7}$$

where t is half wall thickness. Equivalent wall thickness can thus be estimated from the direct measurement of porosity and the estimation of cell length from SEM pictures as

$$t = \frac{l}{2}\left(\frac{1}{\sqrt[3]{\phi}} - 1\right). \tag{8}$$

For example with $l = 220\,\mu$m estimated from SEM micrographs, and $\varnothing = 0.88$, half wall thickness is $t = 4.79\,\mu$m, which is in agreement with the measurements based on SEM micrographs. Use of porosity measurements to determine the wall thickness can be trusted here since the standard deviation on porosity measurements is less than 1%. Therefore, for bimodal foams with 10% and 15% polymer, the cell wall thickness estimate is as follows

$$10\%\ PLA\ Foams: \varnothing = 0.88 \rightarrow t = 4.79\,\mu\text{m},$$

$$Measured\ value\ for\ average\ half\ wall\ thickness \rightarrow t = 4.7\,\mu\text{m},$$

$$15\%\ PLA\ Foams: \varnothing = 0.82 \rightarrow t = 7.52\,\mu\text{m},$$

$$Measured\ value\ for\ average\ half\ wall\ thickness \rightarrow t = 7.5\,\mu\text{m}.$$

The difference between estimated and directly measured values of half cell wall thickness is less than 2%. Due to the simple cell geometry of the fabricated foams, microscopic parameters can be traced right to the actual macroscopic properties, which are directly measured. Therefore, for any desired cell wall thickness, the necessary amount of polymer needed for the cell structure can be calculated.

B. Thermal characteristic length

Thermal length is also a macroscopic geometrical parameter defined as the ratio of twice the fluid volume V_f to the wet surface A.[16] The simplified geometry of PLA foams resulted by the particulate leaching method, makes it possible to analytically derive this parameter based on geometrical properties as shown in Figure 2

$$\Lambda' = \frac{2V_f}{A} = \frac{2l^3}{A_s(1-R_w) + (A_t - A_s)R_w}, \tag{9}$$

where A_s is the total surface of interior cell walls and A_t is the total surface of each cell including the cell wall thickness. In other words, formation of cracks increases the reticulation rate by making openings in the cell wall and, therefore, decreases the wetted wall surface. In parallel, cracks going through the wall, increase the contact surface of the foam structure along the cell wall thickness. Therefore, Eq. (9) becomes

$$\Lambda' = \frac{2l^3}{6l^2(1-R_w) + 6((l+2t)^2 - l^2)R_w} = \frac{2l^3}{6l^2(1-R_w) + 24t(l+t)R_w}. \tag{10}$$

Since cell wall thickness is much smaller than the cell wall length and considering the order of magnitude of l^2 to t, the effect of the surface area caused by cracks is negligible. The added wet surface along the cell wall thickness does not considerably affect the thermal characteristic length. As a result, the second term in the denominator of Eq. (9) has an order of magnitude much lower than the first term and does not affect the overall outcome. On the other hand, foams under study are partially reticulated and R_w is not equal to one anyways, therefore, the following approximation will be used for thermal characteristic length

$$\Lambda' = \frac{2l^3}{6l^2(1-R_w)}. \tag{11}$$

As the reticulation rate increases, the denominator in Eq. (11) diminishes, which results in higher values for thermal characteristic length. With the limit of R_w going to zero,

the thermal length will be equal to $\frac{l}{3} = 73.3\ \mu$m based on cell geometry. This is the lower limit of thermal length and any logical feasible values must be above this limit. Equation (11) can be used to estimate the reticulation rate as

$$R_w = 1 - \frac{l}{3\Lambda'}. \tag{12}$$

From the thermal length values derived by inverse characterization method, reticulation rate can as well be estimated. Estimated values of reticulation rate by Eq. (12) are listed in Table II. It is noteworthy that by adding the water soluble polymer, reticulation rate of the foams increase to more than 31 times the original PLA foams for both 10% and 15% polymer contents. This increase is then leveled off for higher amounts of water soluble polymer.

C. Airflow resistivity

For a porous material with pores of circular cross-sections, flow resistivity is given by[16]

$$\sigma = \frac{8\eta}{\varnothing R^2}. \tag{13}$$

For rectangular pore cross sections, Eq. (13) becomes[16]

$$\sigma = \frac{7\eta}{\varnothing R^2}, \tag{14}$$

where R is the hydraulic radius of pores, η is air viscosity (1.85×10^{-5} Pa.s), and $\varnothing$ is porosity.

For PLA foams, tortuosity does not considerably change with reticulation rate based on inverse characterization results and is only affected by cell wall thickness. To extract the effect of tortuosity, it can be considered as a known value based on the characterization results in the equation describing the flow resistivity as shown in Eq. (14). In the case of PLA foams with rectangular cells, hydraulic radius can be replaced with half-cell length $l/2$. η and $\varnothing$ are not a function of reticulation rate either. Therefore, Eq. (14) can be modified to account for the changes in flow resistivity based on reticulation rate

$$\sigma = E_1 \frac{7\eta\alpha_\infty}{\varnothing R^2} (R_w)^{E_2} = E_1 \sigma' (R_w)^{E_2}. \tag{15a}$$

Here, E_1 and E_2 are the empirical coefficients, which will be evaluated for bimodal PLA foams using the experimental data. Measured values of flow resistivity for different reticulation ratios are plotted in Figure 5. The power equation with the best fit to the experimental data gives the

TABLE II. Estimated values for reticulation rate from theoretical definition of thermal characteristic length.

Foam material	10% PLA	15% PLA
0% PEG	0.0157	0.0958
10% PEG	0.5101	0.4119
20% PEG	0.5601	0.5219
30% PEG	0.5619	0.5408

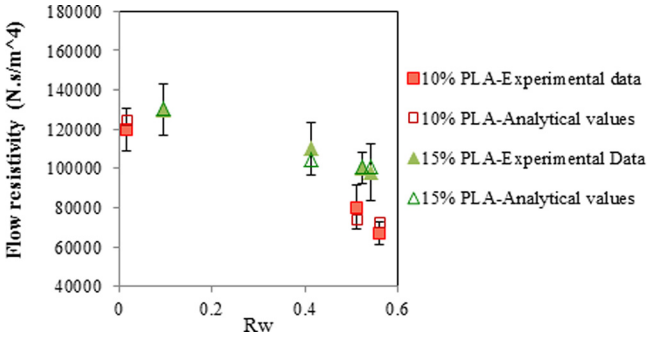

FIG. 5. Comparing the dependency of flow resistivity to reticulation rate, analytical, and experimental values.

analytical values shown in Figure 5 and determines the values of E_1 and E_2 coefficients. As theoretically expected and also observed through experimental results, flow resistivity increases by increasing the cell wall thickness. In Eq. (15a), the effect of cell wall thickness on flow resistivity is imposed by porosity ($\varnothing$). σ' is a function of tortuosity, porosity and cell wall length and can be calculated based on previously measured and derived values for these parameters. Therefore, the value of σ' for each polymer content will be

$$For\ PLA\ foams\ with\ 10\%\ polymer: \quad \sigma' = 14549.8541\ \frac{N.s}{m^4},$$

$$For\ PLA\ foams\ with\ 15\%\ polymer: \quad \sigma' = 19576.4054\ \frac{N.s}{m^4}.$$

Using Eq. (15a), the values of coefficients E_1 and E_2 can be derived from the experimental data. For foams with 10% polymer, Eq. (15a) becomes

$$\sigma = 66955\,(R_w)^{-0.152} = 4.60 \times \sigma' \left(\frac{1}{R_w}\right)^{0.15} \tag{15b}$$

$$\text{and for 15\% polymer}: \sigma = 91755\,(R_w)^{-0.152} = 4.69 \times \sigma' \left(\frac{1}{R_w}\right)^{0.15}. \tag{15c}$$

For Foams with 10% and 15% PLA, the graphs comparing the dependency of flow resistivity to reticulation rate are shown in Figure 5. These graphs include the experimental data as well as analytical values determined by the proposed model. As observed from Figure 5, the two values are very close and Eqs. (15b) and (15c) accurately simulate the dependence of flow resistivity to microstructural properties of bimodal foams. The importance of these two equations is in the fairly close values determined for coefficients E_1 and E_2. Therefore, one unique equation can be derived to link flow resistivity of bimodal foams to its microstructural properties. The fact that identical values were obtained for E_1 and E_2 coefficients proves the validity of Eq. (15a) for the bimodal foam category under study. Developing such equations makes it possible to accurately design any given foam structure to demonstrate certain macroscopic properties by tailoring reticulation ratio and microstructural parameters

$$\sigma = 4.6 \times \sigma' \left(\frac{1}{R_w}\right)^{0.15}. \tag{15d}$$

In Eq. (15d), the effect of cell wall thickness on flow resistivity is applied by σ'; therefore, this equation links flow resistivity to cell wall thickness and reticulation rate.

D. Tortuosity

Dependency of tortuosity to cell geometry has been explained before and tortuosity was found to be constant for different values of reticulation rate in bimodal foams. Figure 6 shows the deviation of characterization results for tortuosity from the estimation. On the other hand, tortuosity was affected by the cell wall thickness and it was determined that tortuosity of 15% PLA foams is 1.5 and for 10% PLA is 1.2. As explained by the following relations:

$$\frac{\alpha_{\infty 15\%}}{\alpha_{\infty 10\%}} = \frac{1.5}{1.2} = 1.25\,. \tag{16a}$$

It is also interesting to note the ratio of square root of cell wall thicknesses

$$\frac{\sqrt{t_{15\%}}}{\sqrt{t_{10\%}}} = \frac{\sqrt{7.52}}{\sqrt{4.79}} = 1.253\,. \tag{16b}$$

It was observed that tortuosity is proportional to the square root of cell wall thickness in partially reticulated open cell foams as expressed by Eq. (16c)

$$\alpha_\infty \propto \sqrt{t}\,. \tag{16c}$$

Obviously more study must be performed to present an analytical equation relating tortuosity to cell wall thickness and Eq. (16c) is only pointing out an observation.

The present biobased foams are specifically fabricated to study the effect of micro structure on macroscopic properties of porous media. To serve this purpose, the particulate leaching method was used to have the utmost control on cellular structure of the porous material. Disadvantage of particulate leaching method is the high flow resistivity of the resulting foams compared to other foaming methods (gas foaming, chemical foaming, etc.). As a result of higher flow resistivity of foams fabricated with lower amounts of water soluble polymer, the standard deviation of acoustic absorption coefficient measurements is higher. Which, in turn, results in increased standard deviation in tortuosity values obtained by inverse characterization method. This explains the larger error bars on the points representing the tortuosity of foams with lower reticulation ratio.

E. Viscous characteristic length

Viscous characteristic length defined by Johnson *et al.*[21] replaces the hydraulic radius in materials with cylindrical pores to account for more general micro geometries.

Johnson *et al.* have defined the characteristic dimension Λ by

$$\Lambda = 2\frac{\int_V v_i^2(r)dV}{\int_A v_i^2(r_w)dA}\,. \tag{17}$$

For a static flow of nonviscous fluid in the porous structure, $v_i(r_w)$ is the velocity of the fluid on the pore surface and the integral in the denominator is performed over the pore surfaces A in the representative elementary volume. The velocity $v_i(r)$ is the velocity inside the pores; the integral in the numerator is performed over the volume V of the pore.[16]

Viscous characteristic length given by Eq. (17) is derived assuming the porous frame to be rigid and it depends only on the geometry of the frame. It has been noted by Johnson *et al.*[21] that Λ and the flow resistivity are related by

$$\Lambda = \frac{1}{c}\left(\frac{7\eta\alpha_\infty}{\sigma\varnothing}\right)^{\frac{1}{2}}. \tag{18}$$

For square cross sectional geometries, coefficient c is obtained by Allard and Atalla[16] to be 1.07. To account for effect of reticulation rate on viscous length, Eq. (18) can be modified to

$$\Lambda = \frac{1}{1.07}\left(\frac{7\eta\alpha_\infty}{\sigma\varnothing}\right)^{\frac{1}{2}} = E_3(R_w)^{E_4}\,, \tag{19a}$$

where E_3 *and* E_4 are coefficients, which will be derived based on experimental data for bimodal PLA foams. Therefore, for different polymer contents, the value of E_3 is

$$\textit{For PLA foams with } 10\%\textit{ polymer}: \; E_3 = 12.811\ \mu\text{m},$$

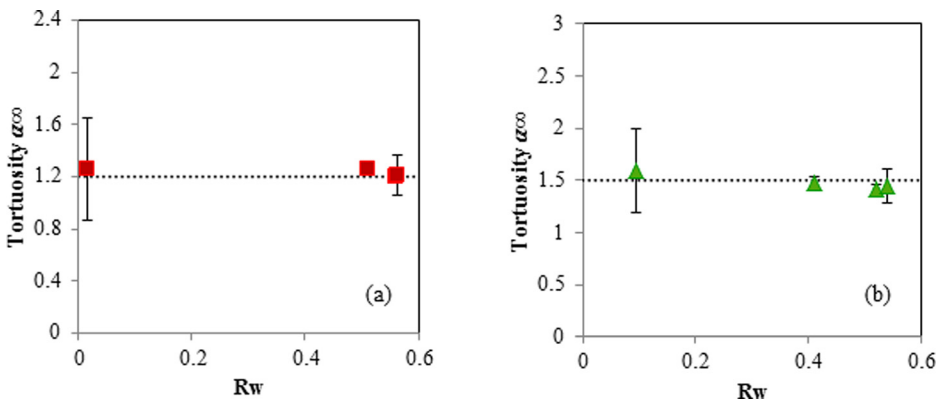

FIG. 6. Tortuosity values for PLA foams with (a) 10% and (b) 15% polymer.

$$For\ PLA\ foams\ with\ 15\%\ polymer:\ E_3 = 9.5237\ \mu m.$$

It is interesting to note that

$$\frac{E_{3\,10\%\,PLA}}{E_{3\,15\%\,PLA}} = \frac{12.811}{9.5237} = 1.345$$

and also the ratio of the previously defined parameter σ' for 15% polymer to that of 10% polymer is equal to

$$\frac{\sigma'_{15\%\,PLA}}{\sigma'_{10\%\,PLA}} = \frac{19576.4054}{14549.8541} = 1.346,$$

which is equal to the ratio of coefficient E_3 for 10% polymer over that of 15% polymer. Therefore, Eq. (19a) for foams with 10% polymer becomes

$$\Lambda = 12.811(R_w)^{0.26} = \frac{186398.18}{\sigma'}(R_w)^{0.26} \tag{19b}$$

and for 15% polymer, we have

$$\Lambda = 9.5237(R_w)^{0.26} = \frac{186439.81}{\sigma'}(R_w)^{0.26}. \tag{19c}$$

Even though the initial coefficients in Eqs. (19b) and (19c) are not equal, when divided by σ' the two coefficients become relatively equal and independent of the polymer content. As a result, a single equation is developed explaining the link between viscous characteristic length and microstructural properties of open cell foam

$$\Lambda = \frac{1.86 \times 10^5}{\sigma'}(R_w)^{0.26}. \tag{19d}$$

As illustrated by Eq. (19d), effect of cell wall thickness is implied by σ' and viscous characteristic length decreases by increasing thickness.[22,23]

Increasing the reticulation rate on the other hand results in growing values for viscous length. The relation between viscous characteristic length and reticulation rate for bimodal foams with 10% and 15% polymer is illustrated in Figure 7. Experimental results are in agreement with the proposed semi analytical equation.

The proposed semi analytical model links microstructural parameters to the macroscopic characteristics of bimodal foams fabricated through this study. These equations provide the means to design the porous cell structure based on any desired macroscopic property to optimize the performance of fabricated open cell foams.

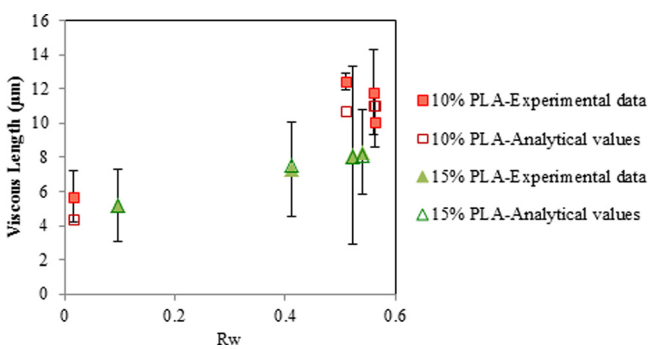

FIG. 7. Comparing the dependency of viscous length to reticulation rate, analytical, and experimental values.

IV. CONCLUSION

In the present study, a semi-empirical model was developed to study the effects of bimodal structure on macroscopic and acoustic properties of porous medium. As the first step, an inverse method based on two microphone impedance tube measurements was applied to eight sets of bimodal PLA foams. This procedure requires direct measurement of open porosity, flow resistivity, and an impedance tube measurement of acoustic absorption coefficient. An inverse characterization of the non-acoustic properties (tortuosity, viscous, and thermal characteristic lengths) is then performed based on Johnson-Champoux-Allard equivalent fluid model to solve an optimization problem. This method adjusts properties in the model to reproduce sound absorption coefficient measurements. Results of inverse method are in good agreement with direct measurements of normal incidence absorption coefficient.

By applying scaling laws to the data collected for bimodal foams, analytical equations were proposed for flow resistivity and viscous characteristic length. These equations link flow resistivity and viscous characteristic length with micro structural parameters such as cell wall thickness and reticulation rate. Although the proposed model is based on fabricated bimodal foams and cannot be applied to various porous structures, this study presents tools to improve the understanding on the effect of microstructure and reticulation rate on the overall acoustical behavior of open cell porous materials.

ACKNOWLEDGMENTS

The authors acknowledge the financial support from the Natural Sciences and Engineering Research Council (NSERC) of Canada, the Canada Research Chairs Program, and the Canada Foundation of Innovation.

[1]D. A. Bies and C. H. Hansen, "Flow resistance information for acoustical design," J. Appl. Acoust. **13**, 357–391 (1980).
[2]M. Garai and F. Pompoli, "A simple empirical model of polyester fiber materials for acoustical applications," J. Appl. Acoust. **66**, 1383 (2005).
[3]N. Kino and T. Ueno, "Experimental determination of the micro and macrostructural parameters influencing the acoustical performance of fibrous media," J. Appl. Acoust. **68**, 1439 (2007).
[4]N. Kino and T. Ueno, "Evaluation of acoustical and non-acoustical properties of sound absorbing materials made of polyester fibers of various cross-sectional shapes," J. Appl. Acoust. **69**, 575 (2008).
[5]N. Kino and T. Ueno, "Comparisons between characteristic lengths and fibre equivalent diameters in glass fibre and melamine foam materials of similar flow resistivity," J. Appl. Acoust. **69**, 325 (2008).
[6]L. J. Gibson and M. F. Ashby, *Cellular Solids—Structure and Properties*, 2nd ed. (Cambridge University Press, Cambridge, 1997/Pergamon, 1988).
[7]C. Perrot, R. Panneton, and X. Olny, "Periodic unit cell reconstruction of porous media: Application to open cell aluminum foams," J. Appl. Phys. **101**, 113538 (2007).
[8]P. Goransson, "Acoustic and vibration damping in porous solids," Philos. Trans. R. Soc. London, Ser. A **364**, 89 (2006).
[9]O. Doutres, N. Atalla, and K. Dong, "Effect of the microstructure closed pore content on the acoustic behavior of polyurethane foams," J. Appl. Phys. **110**, 064901 (2011).

[10]C. Perrot, R. Panneton, and X. Olny, "Computation of the dynamic thermal dissipation properties of porous media by Brownian motion simulation: Application to an open cell aluminum foam," J. Appl. Phys. **102**, 074917 (2007).
[11]C. Perrot, F. Chevillotte, and R. Panneton, "Dynamic viscous permeability of an open cell aluminum foam: Computations versus experiments," J. Appl. Phys. **103**, 024909 (2008).
[12]C. Perrot, F. Chevillotte, and R. Panneton, "Bottom-up approach for microstructure optimization of sound absorbing materials," J. Acoust. Soc. Am. **124**(2), 940 (2008).
[13]L. Boeckx, M. Brennan, K. Verniers, and J. Vandenbroeck, "A numerical scheme for investigating the influence of the three dimensional geometrical features of porous polymeric foam on its sound absorbing behavior," J. Acta Acust. **96**, 239 (2010).
[14]N. J. Mills, "The wet Kelvin model for air flow through open-cell polyurethane foams," J. Mater. Sci. **40**, 5845–5851 (2005).
[15]S. G. Mosanenzadeh, H. E. Naguib, C. B. Park, and N. Atalla, "Development of polylactide open-cell foams with bimodal structure for high acoustic absorption," J. Appl. Polym. Sci. **131**(7), 39518 (2014).
[16]J. F. Allard and N. Atalla, *Propagation of Sound in Porous Media—Modeling Sound Absorbing Materials*, 2nd ed. (Wiley, 2009).
[17]P. C. Lee, H. E. Naguib, C. B. Park, and J. Wang, "Increase of open cell content by plasticizing soft regions with secondary blowing agent," J. Polym. Eng. Sci. **45**(10), 1445–1451 (2005).
[18]P. C. Lee, J. Wang, and C. B. Park, "Extruded open cell foams using two semi-crystalline polymers with different crystallization temperatures," Ind. Eng. Chem. Res. **45**(1), 175–181 (2006).
[19]S. G. Mosanenzadeh, O. Doutres, H. E. Naguib, C. B. Park, and N. Atalla, "A numerical scheme for investigating the effect of bimodal structure on acoustic behavior of polylactide foams," J. Appl. Acoust. **88**, 75–83 (2015).
[20]FOAM-X 2007 User's guide, 2007 ESI GROUP.
[21]D. L. Johnson, J. Koplik, and L. M. Schwartz, "New pore-size parameter characterizing transport in porous media," Phys. Rev. Lett. **57**, 2564–2567 (1986).
[22]E. Ogam and Z. E. A. Fellah, "Recovery of Biot's transition frequency of air-saturated poroelastic media using vibroacoustic spectroscopy," J. Appl. Phys. **116**, 063503 (2014).
[23]M. Sadouki, M. Fellah, Z. E. A. Fellah, E. Oqam, N. Sebaa, F. G. Mitri, and C. Depollier, "Measuring static thermal permeability and inertial factor of rigid porous materials," J. Acoust. Soc. Am. **130**, 2627–2630 (2011).